

Supporting Information

Anisotropic and super-strong conductive hydrogels enabled by mechanical stretching combined with the Hofmeister effect

Bingyan Guo, Yukuan Wu, Shaoshuai He, Changyong Wang, Mengmeng Yao, Qingyu Yu, Xiaojun Wu, Chaojie Yu, Min Liu, Lei Liang, Zhongming Zhao, Yuwei Qiu, Fanglian Yao, Hong Zhang, Junjie Li**

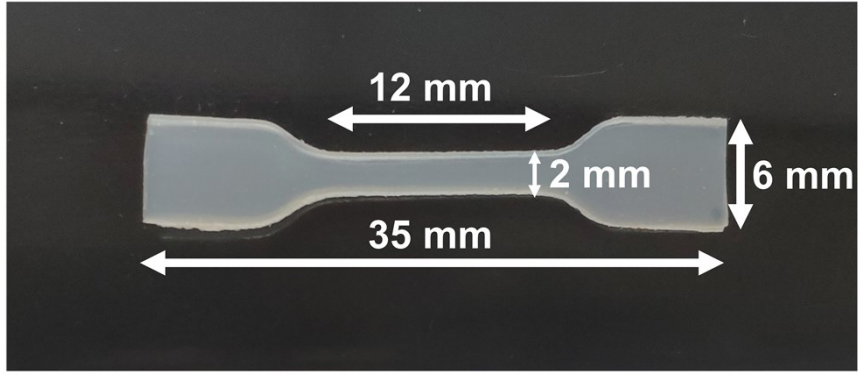


Fig. S1 The dumbbell shape for mechanical tests.

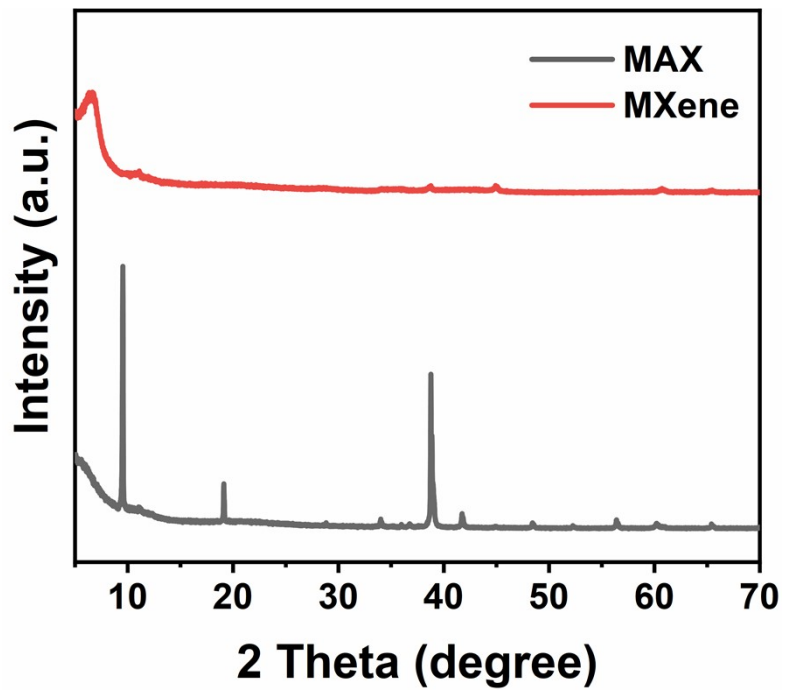


Fig. S2 XRD patterns of Ti_3AlC_2 and $\text{Ti}_3\text{C}_2\text{T}_x$.

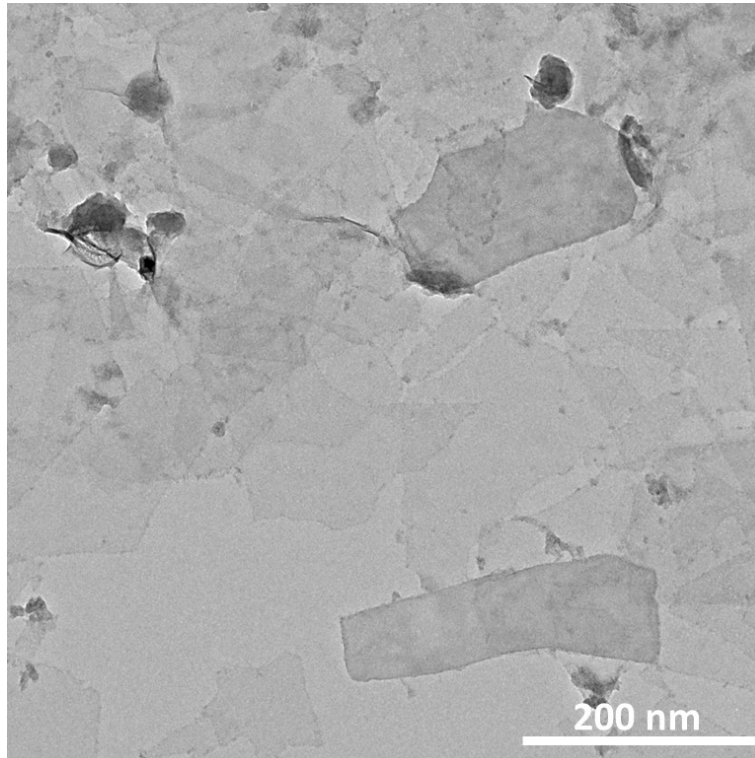


Fig. S3 TEM image of the Ti₃C₂T_x.

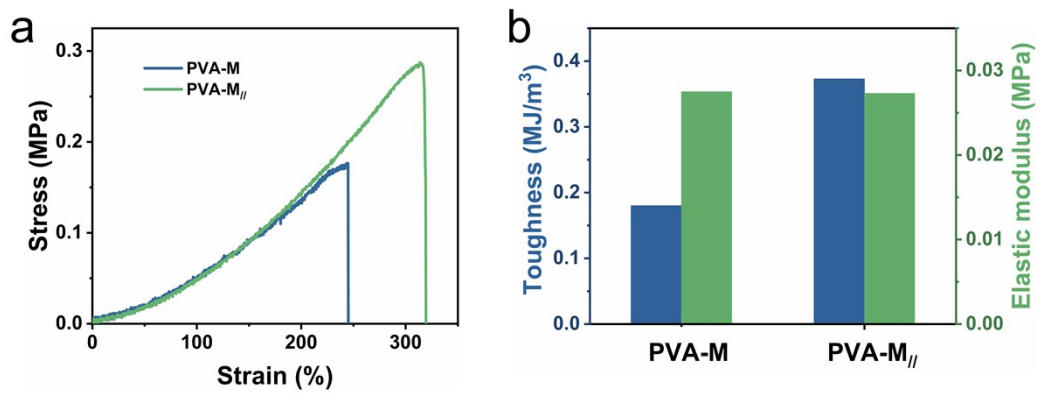


Fig. S4 (a) The tensile stress-strain curves of PVA-M hydrogel and PVA-M_{//} hydrogel. (b) Toughness and elastic modulus of PVA-M hydrogel and PVA-M_{//} hydrogel.

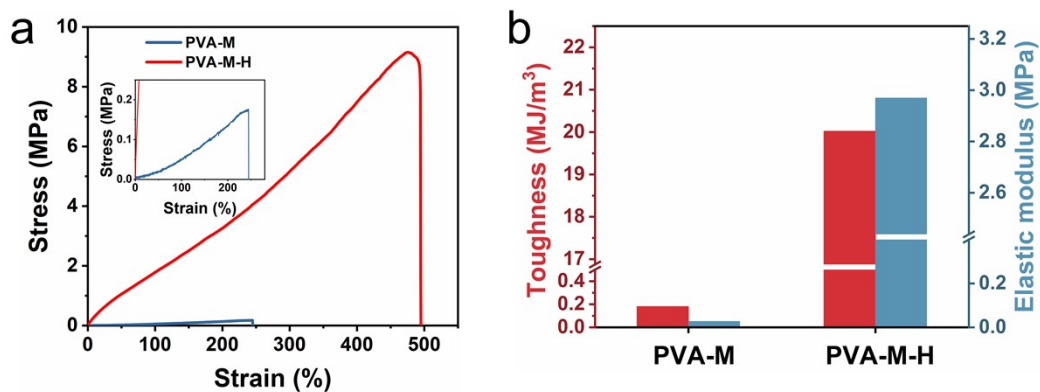


Fig. S5 (a) The tensile stress–strain curves of PVA-M hydrogel and PVA-M-H hydrogel. (b) Toughness and elastic modulus of PVA-M hydrogel and PVA-M-H hydrogel.

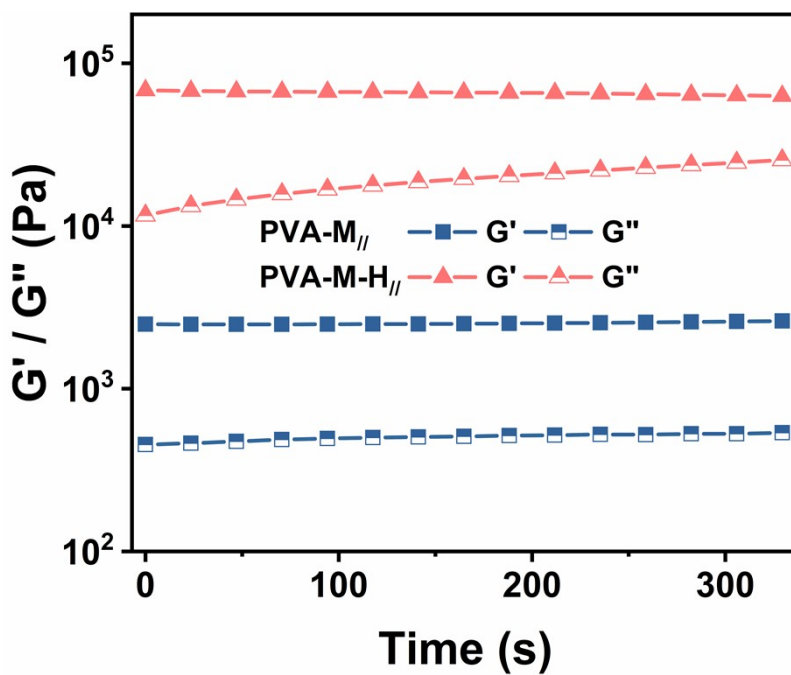


Fig. S6 Rheological behavior of PVA-M_{//} hydrogel before and after immersing in Na₃Cit solution.

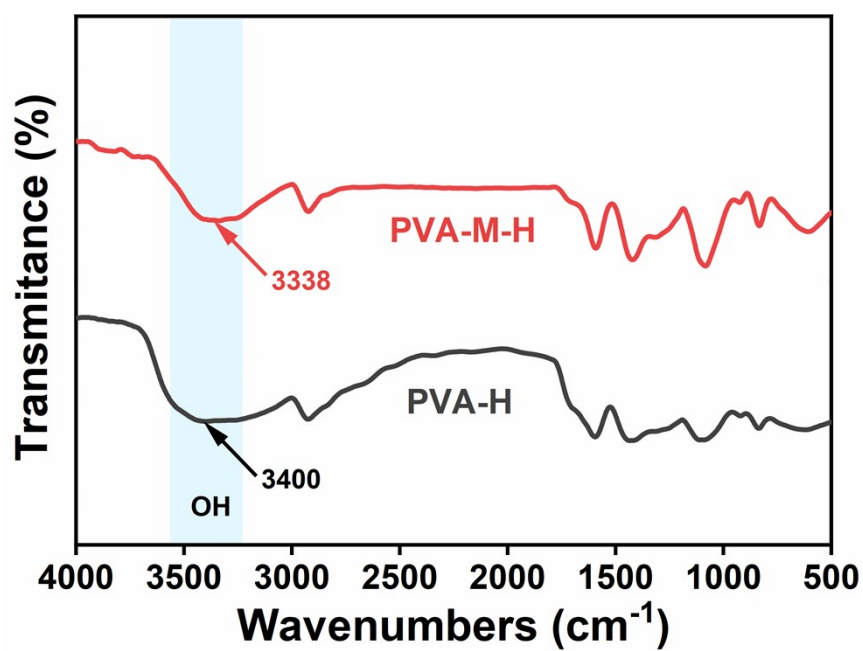


Fig. S7 FTIR spectra of PVA-H hydrogel, and PVA-M-H hydrogel.

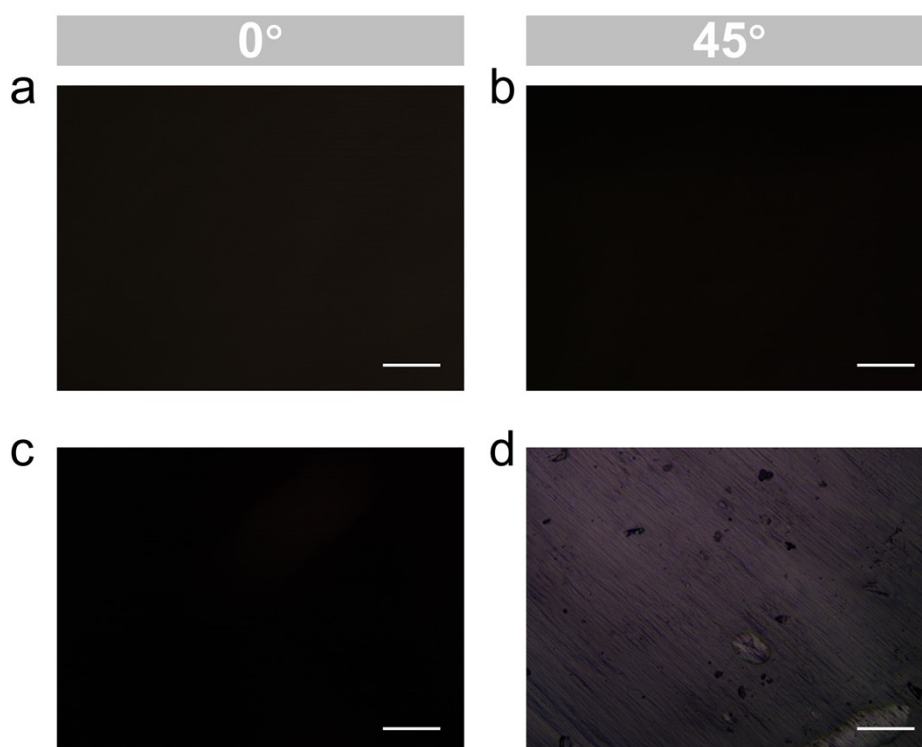


Fig. S8 (a), (b) Polarized microscope images of the isotropic PVA-H hydrogel. (c), (d) Polarized microscope images of the anisotropic PVA-H hydrogel (scale bars: 200 μm).

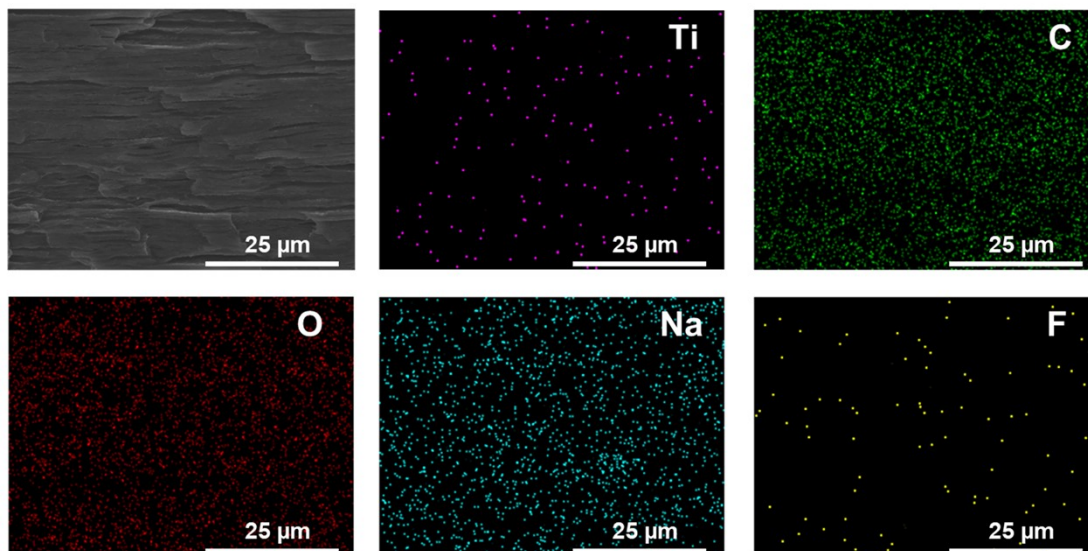


Fig. S9 SEM image and the EDS elemental mapping of Ti, C, O, Na, and F of the cross-sectional of the anisotropic PVA-M-H hydrogel.

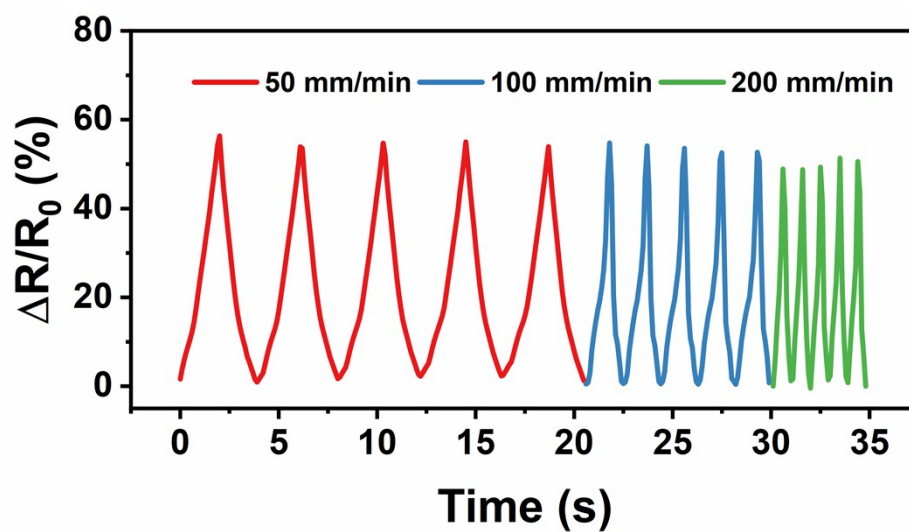


Fig. S10 Relative resistance changes ($\Delta R/R_0$) of PVA-M-H// hydrogel at various stretching rate.

Table S1 Comparison of PVA-M-H_{//} hydrogel to reported tough conductive hydrogels

Materials	Stress (MPa)	Strain (%)	Toughness (MJ/m ³)	Elastic modulus (MPa)	Reference
mechanically trained PVA	5.2	170	N/A	0.2	1
HPC/PVA-NaCl	1.25	800	5.8	0.25	2
PVA-CNF-NaCl	1.4	660	5.25	0.4	3
PVA-Ph/PEDOT	0.8	550	1.1	N/A	4
HA-10PVA	16.1	1,800	200	N/A	5
PVA/NaCl	1.5	550	4.7	0.208	6
PAAm/Ca ²⁺ -Alg	32	62.5	N/A	319	7
P(AGA-co-AAm)-Fe ³⁺	12.1	410	N/A	36.1	8
PAM/MC-As	4.4	690	19.3	3.8	9
DN-Sul-Na	7.5	210	N/A	42.5	10
P(AM-co-AA)/CS	5.1	1225	32.1	1.13	11
s-gel-25%	40	240	N/A	40	12
PACT-P	0.0752	600	N/A	N/A	13
PMZn-GL	0.875	247	0.08	0.001	14
PAC@200%-V	0.55	1585	5.75	0.27	15
PVA-M-H_{//}	16.57	464	39.23	8.58	This work

1. S. Lin, J. Liu, X. Liu and X. Zhao, *Proc. Natl. Acad. Sci. USA*, 2019, **116**, 10244-10249.
2. Y. Zhou, C. Wan, Y. Yang, H. Yang, S. Wang, Z. Dai, K. Ji, H. Jiang, X. Chen and Y. Long, *Adv. Funct. Mater.*, 2019, **29**, 1806220.
3. Y. Ye, Y. Zhang, Y. Chen, X. Han and F. Jiang, *Adv. Funct. Mater.*, 2020, **30**, 2003430.
4. H. Wei, M. Lei, P. Zhang, J. Leng, Z. Zheng and Y. Yu, *Nat. Commun.*, 2021, **12**, 2082.
5. M. Hua, S. Wu, Y. Ma, Y. Zhao, Z. Chen, I. Frenkel, J. Strzalka, H. Zhou, X. Zhu and X. He, *Nature*, 2021, **590**, 594-599.
6. Q. Wang, Q. Zhang, G. Wang, Y. Wang, X. Ren and G. Gao, *ACS Appl. Mater. Interfaces*, 2022, **14**, 1921-1928.
7. W. Cui, M. Pi, R. Zhu, Z. Xiong and R. Ran, *J. Mater. Chem. A*, 2021, **9**, 20362-20370.
8. V. T. Tran, M. T. I. Mredha, S. K. Pathak, H. Yoon, J. Cui and I. Jeon, *ACS Appl. Mater. Interfaces*,

2019, **11**, 24598-24608.

9. W. Chen, D. Li, Y. Bu, G. Chen, X. Wan and N. Li, *Cellulose*, 2020, **27**, 1113-1126.
10. X. Sun, Y. Liang, L. Ye and H. Liang, *J. Mat. Chem. B*, 2021, **9**, 7751-7759.
11. Y. Liang, L. Ye, X. Sun, Q. Lv and H. Liang, *ACS Appl. Mater. Interfaces*, 2020, **12**, 1577-1587.
12. P. Lin, T. Zhang, X. Wang, B. Yu and F. Zhou, *Small*, 2016, **12**, 4386-4392.
13. W. Wang, X. Deng and C. Luo, *J. Mater. Chem. C*, 2023, **11**, 196-203.
14. Y. Feng, H. Liu, W. Zhu, L. Guan, X. Yang, A. V. Zvyagin, Y. Zhao, C. Shen, B. Yang and Q. Lin, *Adv. Funct. Mater.*, 2021, **31**, 2105264.
15. L. Chen, X. Chang, J. Chen and Y. Zhu, *ACS Appl. Mater. Interfaces*, 2022, **14**, 43833-43843.